

The spectroscopic binary system Gl 375[★]

I. Orbital parameters and chromospheric activity

R. F. Díaz¹, J. F. González², C. Cincunegui¹, and P. J. D. Mauas¹

¹ Instituto de Astronomía y Física del Espacio (IAFE), CC. 67, suc. 28, 1428 Buenos Aires, Argentina
e-mail: rodrigo@iafe.uba.ar

² Complejo Astronómico El Leoncito (CASLEO), San Juan, Argentina

Received 30 June 2007 / Accepted 8 August 2007

ABSTRACT

Aims. We study the spectroscopic binary system Gl 375 to characterise its orbit and the spectral types and chromospheric activity levels of the components.

Methods. We employed medium-resolution *echelle* spectra obtained at the 2.15 m telescope at the Argentinian observatory CASLEO and photometric observations obtained from the ASAS database.

Results. We have separated the composite spectra into those corresponding to both components. The separated spectra allow us to confirm that the spectral types of both components are similar (dMe3.5) and to obtain precise measurements of the orbital period ($P = 1.87844$ days), minimum masses ($M_1 \sin^3 i = 0.35 M_\odot$ and $M_2 \sin^3 i = 0.33 M_\odot$), and other orbital parameters. The photometric observations exhibit a sinusoidal variation with the same period as the orbital period. We interpreted this as signs of active regions carried along with rotation in a tidally synchronised system, and studied the evolution of the amplitude of the modulation on longer timescales. Together with the mean magnitude, the modulation exhibits a roughly cyclic variation with a period of around 800 days. This periodicity is also found in the flux of the Ca II K lines of both components, which seem to be in phase.

Conclusions. The periodic changes in the three observables are interpreted as a sign of a stellar activity cycle. Both components appear to be in phase, which implies that they are magnetically connected. The measured cycle of ≈ 2.2 years (≈ 800 days) is consistent with previous determinations of activity cycles in similar stars.

Key words. binaries: spectroscopic – stars: activity – stars: chromospheres – stars: flare – stars: fundamental parameters – stars: late-type

1. Introduction

The $V = 11.27$, $B - V = 1.56$ (Perryman et al. 1997) spectroscopic binary system, Gl 375 (V* LU Vel, HIP 48904), is located 16 pc away in the southern constellation Vela, at RA (J2000) = 09:58:34 and Dec (J2000) = $-46:25:30$. Both components of the system exhibit high levels of chromospheric emission.

Until recently, the duplicity of the system and its high level of chromospheric activity were both unknown. Although a considerable number of photometric measurements exist in the literature, including very early works (see for example Kron et al. 1957; Corben et al. 1972; Doyle & Butler 1990; Bessel 1990), the flare activity of Gl 375 was only discovered in a relatively recent work by Doyle et al. (1990) using optical spectroscopy and optical and infrared photometry. They reported a high rate of flare occurrence and classified Gl 375 as dM3.5e. Bidelman (1985) reported the same spectral classification for the system but did not indicate the presence of emission lines. The spectral resolution of Doyle et al. (1990) was not high enough to resolve the double features in the spectra of Gl 375, but they noted that the FWHM of the H_α line was twice that found in the spectra of a similar star. Therefore, they concluded that Gl 375

was either a fast rotator or a binary. Only recently have Christian & Mathioudakis (2002) obtained a high-resolution optical and IR spectrum of Gl 375, which allowed them to identify the characteristic double features and report the binary nature of this object.

Stars in close binary systems tend to show higher levels of activity than single stars with the same characteristics (see, for example Schrijver & Zwaan 1991; Zaqarashvili et al. 2002). Due to its vicinity and relative brightness, the present system constitutes an interesting opportunity for studying two very active stars in interaction.

The $\alpha\Omega$ dynamo is usually accepted as the cause of activity cycles in late-type stars with an outer convective layer. This dynamo is thought to be the result of the differential rotation at the interface between the convective envelope and the radiative core. Therefore, the presence and characteristics of activity cycles are closely related to the existence and depth of an outer convection zone. Since this depth depends on spectral type – from F stars that have shallow convection zones to middle M stars that are totally convective – it is especially interesting to study these cycles in stars of different spectral types and, in particular, in middle-M stars, to determine whether there is an onset of cyclic activity. Recently, an activity cycle has been detected in Proxima Centauri (Cincunegui et al. 2007a). To our knowledge, this is the only fully convective M-type star for which an activity cycle has been detected so far, and it poses a question on the origin of such a cycle.

[★] The authors are visiting astronomers of the Complejo Astronómico El Leoncito, operated under an agreement between the Consejo Nacional de Investigaciones Científicas y Técnicas de la República Argentina and the National Universities of La Plata, Córdoba, and San Juan.

Table 1. Observation log for Gl 375.

Date ^a	HJD ^b	Exp time [s]	Orbital phase	Notes ^c
020399	1 241.6469	4200	0.3572	§
030399	1 242.5470	3000	0.8363	
210300	1 626.5748	9600	0.2756	
220300	1 627.5486	9540	0.7940	!a
040301	1 973.6596	14 400	1.0480	
040701	2 095.4968	2400	0.9087	
021201	2 246.7938	9600	0.4525	
300302	2 364.5754	6000	1.1541	
250602	2 451.4672	4800	0.4115	
160303	2 715.6247	6000	1.0371	
130603	2 804.4781	2400	0.3387	
071203	2 981.8507	6000	0.7639	!a
090304	3 074.6662	6000	1.1747	
030604	3 160.5119	6000	0.8752	
251104	3 335.8051	1200	0.1934	!
190305	3 449.6718	6000	0.8110	!
231105	3 698.8419	7200	0.4580	
241105	3 700.8344	6000	0.5187	
120206	3 779.7498	9600	0.5297	

^a In *ddmmyy* format. ^b HJD-2 450 000. ^c See Sect. 4.3.

The recent discovery of a 5 Earth-mass planet in the habitable zone of the M3 dwarf Gl 581 (Udry et al. 2007) has made the study of habitability in these stars increasingly relevant (see, for example, Buccino et al. 2006, 2007; von Bloh et al. 2007). Changes in the rate of flare occurrences and CMEs characteristic of activity cycles could in principle affect the habitability of a planet in close orbit.

Gl 375 was observed as part of an ongoing programme to study chromospheric activity in late-type main sequence stars. By the time of our first observations in the year 1999, its binary nature was unknown. However, it was quickly realised that this was a double system, with strong chromospheric emission that was similar in both components.

In this first paper we present medium-resolution spectra of Gl 375 spanning more than six years. We obtained precise measurements of the orbital parameters of the system and find evidence of an activity cycle in both components. In Sect. 2 we describe the spectroscopic observations and outline the reduction procedure. In Sect. 3 we describe the method used to separate the spectra of each component and present precise measurements of the orbital parameters of the system. In Sect. 4 we analyse photometric and spectroscopic data of Gl 375 and find periodic variations consistent with an activity cycle. Finally, in Sect. 5 we summarise our results and outline our conclusions.

2. Observations and data reduction

The spectroscopic observations were obtained using the REOSC spectrograph in the Jorge Sahade 2.15 m telescope at the Complejo Astronómico El Leoncito (CASLEO), located 2550 m above sea level in the Argentinian Andes. The spectra cover the entire optical range (from ≈ 3800 to 6800 \AA) in 24 *echelle* orders. We employed a 300 micron-width slit that provided a resolving power of $R = \lambda/\delta\lambda \approx 13\,200$. The detector used was a 1024×1024 pixel TEK CCD camera.

Observations began in 1999 and are still going on. We obtain about three observations a year, weather permitting. A log of the observations analysed here is presented in Table 1. Each log entry actually consists of two individual observations that

are combined to remove cosmic rays, and the reported exposure time is the sum of the exposure times of the two individual observations. The individual spectra are used in Sect. 4.3 to look for flares in the observations.

The observations were reduced and analysed using standard IRAF¹ routines. We calibrated the spectra in flux, using low-dispersion, long-slit spectra of the same star. For details of the reduction and flux-calibration process, we refer the reader to Cincunegui & Mauas (2004). The resulting spectral resolution is high enough to clearly resolve the double features in the spectra of Gl 375 at appropriate phases. The exposure times ranged from 20 min to 240 min, producing a wide range of S/N.

Our spectral coverage allows us to study the effect of chromospheric activity in the whole optical spectrum simultaneously. In previous works we have studied the behaviour of different lines in our complete stellar sample (see Cincunegui et al. 2007b, for the H & K Ca II lines and H α ; Díaz et al. 2007, for the Na I D lines; and Buccino & Mauas 2007, for the Mg II *h* and *k* UV lines).

3. Spectra separation and orbital parameters

The composite spectra were separated using the iterative method presented by González & Levato (2006). This method allows computation of the individual spectra and the radial velocities (RVs) of the two stellar components of the binary system. In each iteration the computed spectrum of one component is used to remove its spectral features from the observed spectra. The resulting single-lined spectra are then used to measure the RV of the remaining component and to compute its spectrum by combining them appropriately.

As a template for the cross-correlations, we used a spectrum of a star of similar spectral type (AD Leo = Gl 388) observed with the same instrumental setup during the night of March 7, 2004. The zero-point was established with an uncertainty of about 0.5 km s^{-1} by means of the observation of RV standard stars. In all cases for RV measurements, we excluded the emission lines.

A mean spectra of very high S/N was obtained for each component, which were used to check the spectral type of the stars. These spectra are shown in Fig. 1, together with the spectrum of AD Leo we employed. As can be seen, the three spectra are remarkably similar, indicating that both the primary and secondary components of Gl 375 have spectral type M3.5Ve. To measure the spectral type of the components, we employed the TiO bands used by Pettersen & Hawley (1989) to compute the intrinsic brightness of a sample of red flare stars. Unfortunately, only three of these bands fall within our spectral range (4760 \AA , 4950 \AA , 5450 \AA). We carefully compared the strength of these bands in the mean spectra of each component and in AD Leo and found that both stars are very similar between them and similar to AD Leo, one of the dM3.5 stars used by Pettersen & Hawley (1989). Therefore, the spectral types of the components must be around M3.5. Additionally, we computed the absolute magnitude of each component using the parallax from the Hipparcos catalogue (Perryman et al. 1997) and taking into account our result that both stars are identical. We found that both components have an absolute magnitude of $M_v = 11.01$, which is in excellent agreement with the value for AD Leo $M_v = 10.98$ (see

¹ IRAF is distributed by the National Optical Astronomy Observatories, which are operated by the Association of Universities for Research in Astronomy, Inc., under cooperative agreement with the National Science Foundation.

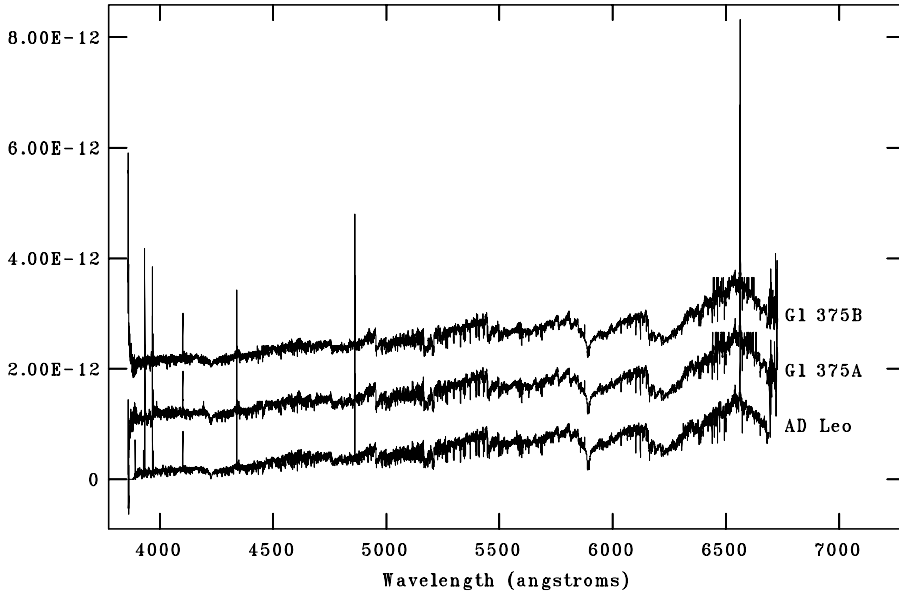


Fig. 1. Mean spectra of the two components of the binary system Gl 375, together with the spectrum of AD Leo used as template. The entire observed spectral range is shown, and the spectra are displaced for clarity.

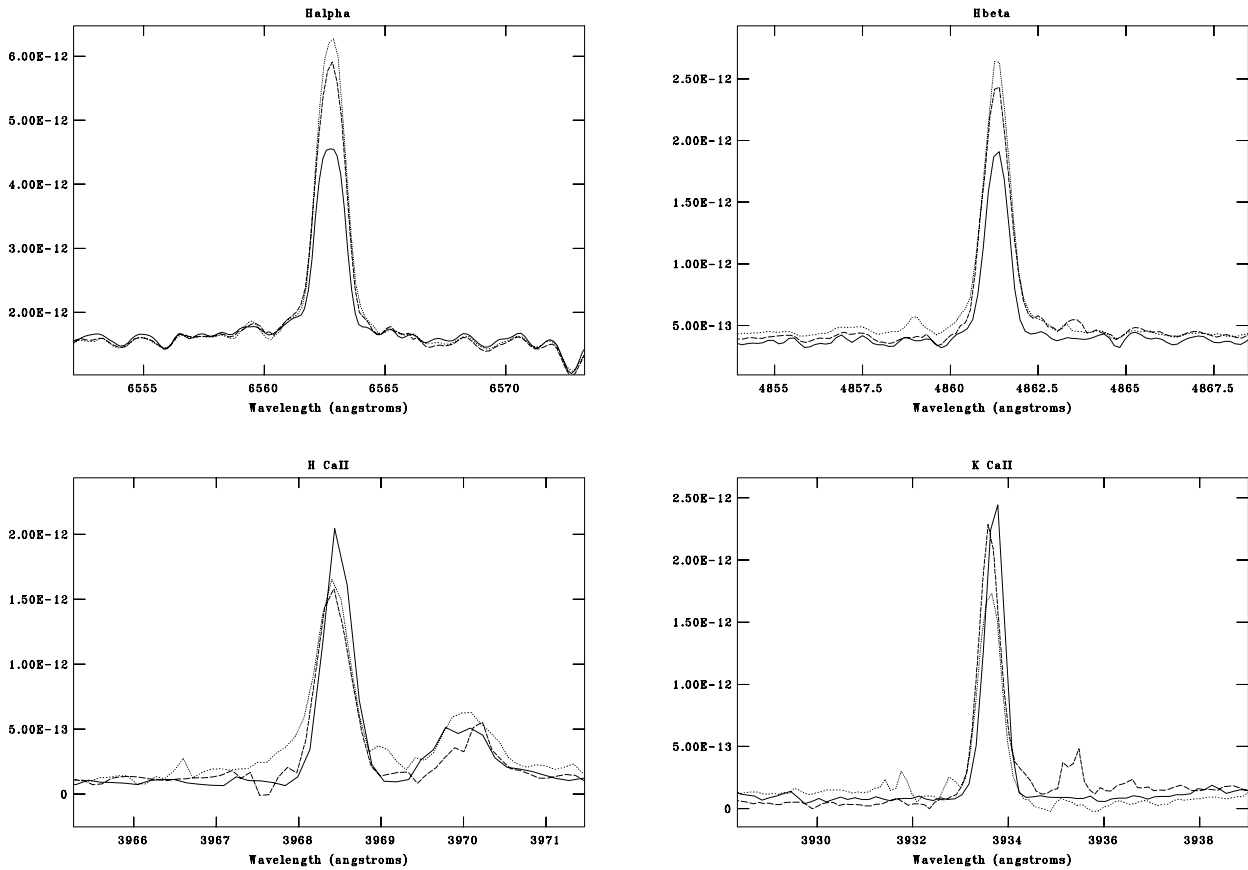


Fig. 2. Comparison of the $H\alpha$, $H\beta$, Ca II H, and Ca II K line emissions in AD Leo (solid line), Gl 375A (dashed line), and Gl 375B (dotted line). The spectra of Gl 375 are mean spectra obtained from the entire set of observations.

Johnson 1965; van Altena et al. 1995). Unfortunately, we could not verify the obtained spectral type directly by using the relations given by Reid et al. (1995) and Kirkpatrick et al. (1991), since the TiO bands employed in those papers lie outside our spectral range.

Also evident from Fig. 1 is the high level of emission in the Balmer lines and in the H & K Ca II lines, which implies a high level of chromospheric activity. In Fig. 2 we compare the flux

intensity of AD Leo and Gl 375 in $H\alpha$, $H\beta$, and in the Ca II H & K lines. Note that the line intensities in the mean spectra of Gl 375A and Gl 375B are comparable to those from AD Leo, which is considered a very active flare star. This should be expected since, as mentioned in the introduction, stars in close binary systems usually exhibit enhanced levels of chromospheric activity when compared with single stars with the same characteristics (Schrijver & Zwaan 1991; Zaqarashvili et al. 2002).

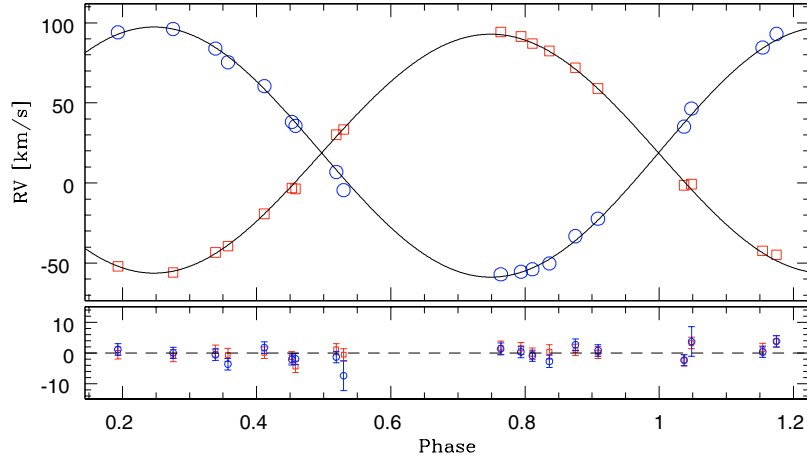


Fig. 3. RVs measurements phased to the orbital period $P = 1.8784425$ days. The squares represent measurements of the primary star and the circles are measurements of its companion. The solid line is the best fit to the data. In all cases, the error bars are smaller than the symbols. In the lower panel we show the residuals of the fit and the individual errors.

In Sect. 4.3 we present evidence of a continuous interaction between the magnetospheres of the components that may lead to an enhanced level of chromospheric activity.

Using the obtained values of RV, we fit a Keplerian orbit to the system. In Fig. 3 we show the RV curves along with the resulting fit. The orbital parameters we obtained are presented in Table 2. Note that the orbital inclination angle cannot differ much from 90° , since the minimum mass of the components is close to the expected value for M-type dwarves, which is around $0.4 M_\odot$ for spectral type M2 and $0.22 M_\odot$ for M5 (Cox 2000). Therefore the minimum distance $a \sin i = (5.665 \pm 0.035) R_\odot$ should be similar to the actual separation between the components. For such a tight orbit, we would expect to find the stars tidally locked. In this respect, Zahn (1977) studied the effects of turbulent viscosity in binary star systems and provided expressions for the characteristic time for orbital and rotational synchronisation and orbital circularisation. Employing Eqs. (6.1) and (6.2) from that work, we find that for a system like the one studied here, the synchronisation time is

$$t_{\text{sync}} \approx (q)^{-2} (a/R_1)^6 \approx 8.9 \text{ Myr}$$

and the circularisation time is

$$t_{\text{circ}} \approx (q(1+q)/2)^{-1} (a/R_1)^8 \approx 1.7 \text{ Gyr},$$

where $q = M_2/M_1$ and R_1 is the radius of the primary. For these calculations we assumed the primary radius to be $0.4 R_\odot$ (see Cox 2000) and the orbital separation to be similar to its minimum value, $a \approx 5.66 R_\odot$. Therefore, since we found a value of the eccentricity that is undistinguishable from zero, we believe the system must have its orbital and rotational periods synchronised. However, to our knowledge no measurements of the period of rotation of this system exist in the literature. In Sect. 4.2 we provide more evidence that the rotational and orbital periods are indeed synchronised.

4. Variability

In this section, we study the variability of Gl 375 as a whole and of each component. Besides using the spectra obtained at CASLEO, we also employed photometric observations provided by the All Sky Automated Survey (ASAS, Pojmanski 2002). The ASAS data for this system cover the period between 2002 and

Table 2. Orbital parameters for Gl 375.

Conjunction epoch [HJD]	2452779.422 ± 0.005
Period [days]	1.87844246 ± 0.0000049
$a \sin i [R_\odot]$	5.665 ± 0.035
Systemic velocity [km s^{-1}]	18.81 ± 0.32
Primary RV amplitude [km s^{-1}]	74.58 ± 0.68
Secondary RV amplitude [km s^{-1}]	78.07 ± 0.66
Orbital eccentricity	0.0072 ± 0.0070
$M_1 \sin^3 i [M_\odot]$	0.3541 ± 0.0068
$M_1 [M_\odot]$	$>0.3646^a$
$M_2 \sin^3 i [M_\odot]$	0.3382 ± 0.0068
$M_2 [M_\odot]$	$>0.3482^a$

^a Inferred from the absence of eclipses in the lightcurve.

2006, with gaps during the year 2002 and 2005. We discarded all the observations that were not qualified as either A or B in the ASAS database (i.e. we retained only the best-quality data), as well as 7 outlier observations. The final dataset consists of 295 points, with typical errors of around 15 mmag.

4.1. Mean magnitude

In Fig. 4 we plot the mean V magnitude of the system as a function of time, as measured by ASAS. The empty squares represent the weighted mean of the observations, taken over four months in each observing season, and the error bars represent the square root of the variance of the weighted mean, computed as (see Frodesen et al. 1979, Eq. (9.12))

$$\text{Var} = \left(\sum_{i=1}^n 1/\sigma_i^2 \right)^{-1},$$

where σ_i is the photometric error of i th point, which is provided by ASAS, and n is the total number of observations analysed. Note the lack of observations during part of the 2002 season, as well as in all of 2005 and the beginning of 2006.

A maximum is discernable around the year 2002.5 (HJD ≈ 2452430) and a minimum in 2004 (HJD ≈ 2453050). A few additional minima seem to be present near 2002 (HJD ≈ 2452200) and 2003.25 (HJD ≈ 2452700). Unfortunately, the lack of observations during the last part of 2004 and 2005

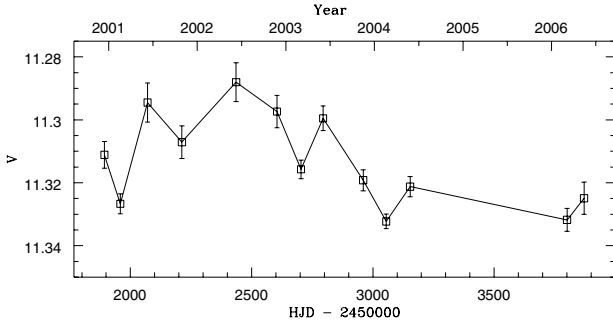


Fig. 4. Mean V magnitude of Gl 375 as measured by the All Sky Automated Survey as a function of time. The mean was taken every four months in each observing season.

precludes any further analysis at this point, since a maximum could have occurred in 2005. We return to this issue in Sect. 4.3.

4.2. Rotational modulation

We calculated the Lomb-Scargle periodogram (Scargle 1982; Horne & Baliunas 1986) for the ASAS data. This periodogram is a method of estimating the power spectrum (in the frequency domain), when observation times are unevenly spaced, and it normalises the spectrum in such a way that it is possible to estimate the significance of the peaks. The amplitude of the periodogram at each frequency point is identical to the equation that would be obtained when estimating the harmonic content of a data set at a given frequency, by linear least-square fitting to an harmonic function of time (Press et al. 1992). We show this periodogram in Fig. 5.

As can be seen, there is a distinct peak corresponding to a period of $P_{\text{phot}} = 1.876644$ days. For this peak, the false alarm probability is about 0.1%. The excellent false alarm probability indicates the presence of a harmonic variability within the data set with a period resembling the measured orbital period very closely.

We believe this harmonic variability is produced by spots and active regions in the stellar surface carried along with rotation. This would imply that the rotational and orbital periods are synchronised, as is expected for such a close binary.

To verify if this is indeed the case, we phased the data to the obtained period for two different seasons (Fig. 6). The sinusoidal shape of the variation is evident, although the amplitude of the modulation is different in both cases: between 2002.5 and 2003.5 (upper panel), the amplitude is about 30 mmag and falls to about 15 mmag during 2006. This could indicate a different area covered by starspots or active regions, therefore different activity levels, in each epoch. Note that during the period of minimum modulation the mean brightness is smaller by about 20 mmag.

Note also that whether the period of maximum rotational modulation corresponds to an epoch of maximum or minimum activity depends on the filling factor. On the other hand, the variations in the mean brightness can be dominated by the active regions (as in the Sun) or by the spots (as in younger stars), which would cause the stars to be either brighter or fainter during periods of maximum activity, respectively. Therefore, considering that the observed system is fainter during the period of minimum modulation (see Fig. 6), we are left with two possibilities. Either the system is dominated by active regions and the filling factor during maximum activity is below 50% (as in the Sun) or the spots control the photometric variations and the maximum filling factor is over 50%.

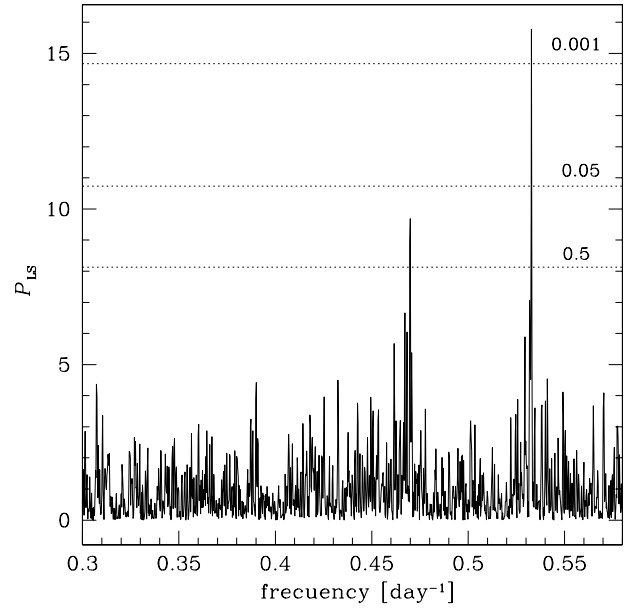


Fig. 5. Lomb-Scargle periodogram of the ASAS data. The main peak occurs at $P_{\text{phot}} = 1.876644$ days and has a false alarm probability of about 0.1%. The horizontal dashed lines show the values of the false alarm probability.

We found no evidence of eclipses in the photometry. Since the ASAS data have complete phase coverage in many periods, this could not be an eclipsing system, so we can set an upper limit to the inclination angle. Assuming a stellar radius of $0.4 R_{\odot}$ for both components, the inclination angle should be larger than 82° . In turn, this implies lower limits for the stellar masses $M_1 > 0.3646 M_{\odot}$ and $M_2 > 0.3482 M_{\odot}$. Note that the assumed spectral type of the stars remain consistent with these values.

To study the evolution of the activity level, we studied the changes in the amplitude of the photometric modulation as a function of time in greater detail. Assuming that the modulation is produced by active regions and spots in the stellar surface, its amplitude should trace the amount of inhomogeneities at the surface, and hence trace the level of magnetic activity.

We binned the ASAS measurements every four months and phased the data for each bin to the orbital period. Bins in which less than 7 observations were present were discarded. The phased data was then fitted to a sinusoidal model of the form

$$a_0 + a_s \sin(2\pi\varphi) + a_c \cos(2\pi\varphi), \quad (1)$$

where φ is the orbital phase. The resulting fit parameters and their covariance matrix were employed to measure the amplitude A of the variation and its standard error σ_A in every time bin:

$$A = \sqrt{a_s^2 + a_c^2} \quad (2)$$

$$\sigma_A = A^{-1}[\text{var}(a_s) a_s^2 + \text{var}(a_c) a_c^2 + 2 a_s a_c \cdot \text{cov}]^{1/2}, \quad (3)$$

where $\text{var}(a_x)$ denotes the variance of the parameter a_x and cov is the covariance of the parameters. The results are shown in Fig. 7, where the time assigned to each measurement was the mean time of the photometric data considered.

It is interesting to compare the present figure with Fig. 4. The rotational modulation also exhibits a maximum around the year 2002.5, as in the previous section, and there are also two marked minima around the years 2002 and 2004, although the minima in the amplitude of the rotational modulation are more

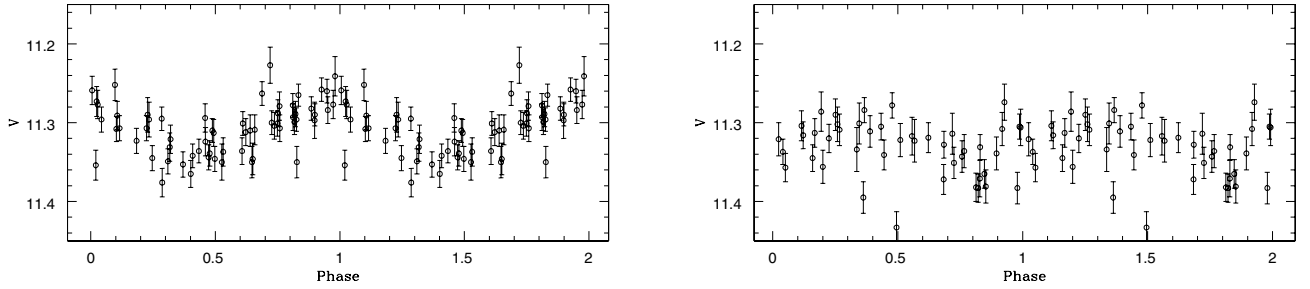


Fig. 6. ASAS photometry phased to the orbital period for two different epochs. *Left:* 2002.5–2003.5 *Right:* 2006.

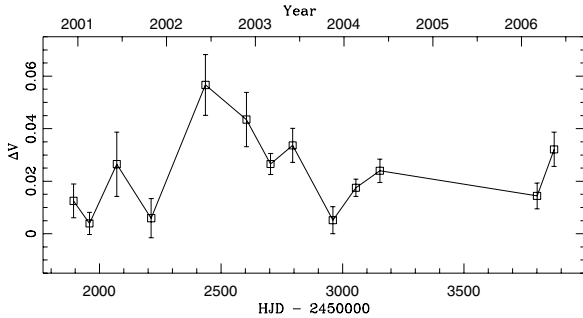


Fig. 7. Variation in the binned photometric data as measured from a sinusoidal fit (see text) as a function of time. A peak is clearly visible near the year 2003.

significant. Consider that, although these measurements originate in the same dataset, the presence of minima and maxima at the same time is meaningful, since the measurements are of different natures.

4.3. Magnetic activity

To study the magnetic activity of the system, we use the flux in the CaII K line, a well-known activity indicator. We did not use the CaII H line, since it is contaminated by the nearby Balmer line H ϵ , which we expect to be in emission in these active stars.

Since we have separated the spectra from both components, we should be able to distinguish whether the changes observed in the photometric measurements belong to one of the components or to both. The spectroscopic measurements also provide more information about the active regions present at the stellar surfaces. For example, combining the photometric data with measurements of activity proxies, it should be possible to discern whether active regions or stellar spots dominate the photometric variations and whether the filling factor is larger or smaller than 50%. Furthermore, since we have observations for the year 2005, a more detailed study of the system variability is possible.

We carefully examined the separate spectra and discarded those where reduction problems were present or where the S/N was too poor. We also discarded spectra that exhibited signs of a transient event, such as a flare. To do this we employed the individual observations (see Sect. 2) and compared the amplitudes of the K line fluxes in one individual spectrum with those in the other. If no flare were present, no significant difference should be observed, since the time between observations is about an hour. On the other hand, if a strong transient event is present during our observations, we should observe differences in the K line fluxes from one spectrum to the next. In the last column of Table 1, the discarded observations are marked with a ! sign. In some cases, generally due to changing weather conditions or

Table 3. Flux in the Ca II K line for both components of the system.

Name	HJD-2 450 000	f (primary)	f (secondary)
		[10^{-13} ergs cm $^{-2}$ Å $^{-1}$ s $^{-1}$]	
030399	1 242.5470	10.48	9.24
210300	1 626.5748	10.41	7.71
220300	1 627.5486	12.62	12.76
040301	1 973.6596	10.57	9.50
040701	2 095.4968	4.35	4.07
021201	2 246.7938	7.89	7.25
300302	2 364.5754	10.86	9.46
250602	2 451.4672	8.51	9.91
160303	2 715.6247	10.83	8.20
130603	2 804.4781	5.06	3.28
071203	2 981.8507	13.44	11.84
090304	3 074.6662	9.26	7.82
030604	3 160.5119	8.87	9.11
231105	3 698.8419	1.40	1.65
241105	3 700.8344	4.97	3.42
120206	3 779.7498	3.43	2.05

the presence of flares, only one of the individual spectra had to be discarded. In those cases, a letter next to the sign indicates which spectra was discarded, either a or b, for the first and second ones, respectively. Additionally, the spectra taken during the night of March 2, 1999 (marked §) were discarded because the spectral range does not include the Ca II K line, due to the use of a different instrumental setup during that night. The flux measurements were carried out in the remaining individual spectrum, after checking that the regions of interest were free of cosmic rays. Unfortunately, one of the discarded spectra belong to the year 2005 and another one to the end of 2004.

The fluxes in the K line were computed in a 1 Å window using the IRAF task SBANDS, which measures the flux by summing each pixel in the defined interval. At the edges of the bandpass, it considers only the fraction of the pixel within the bandpass. The results are presented in Table 3. In Fig. 8 we plot the K line flux for both components of the system. The error in the line fluxes was conservatively estimated as 10%. It can be seen that the fluxes are strongly correlated ($r = 0.95$) and the activity variations of the components should therefore be in phase. For this to occur, the magnetospheres of the stars must be strongly interacting. Vahia (1995) simulated the interaction of the magnetic field of binary stars. In that work, the stars are modelled as perfect dipoles surrounded by vacuum, and it is shown that it should be quite common to find one of the components located completely inside the magnetosphere of the other. Various works describe mechanisms by which magnetic activity can be enhanced in interacting systems like this one (see, for example, Zaqarashvili et al. 2002). This kind of mechanism could in principle explain the high level of emission present in the lines used

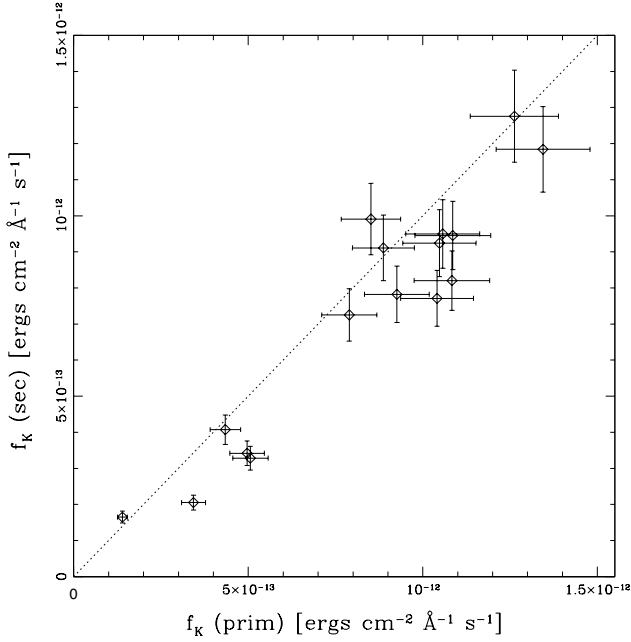


Fig. 8. Comparison of the fluxes in the Ca II K line for both components. The error bars correspond to a 10% error in the line fluxes, and the dotted line is the identity relation.

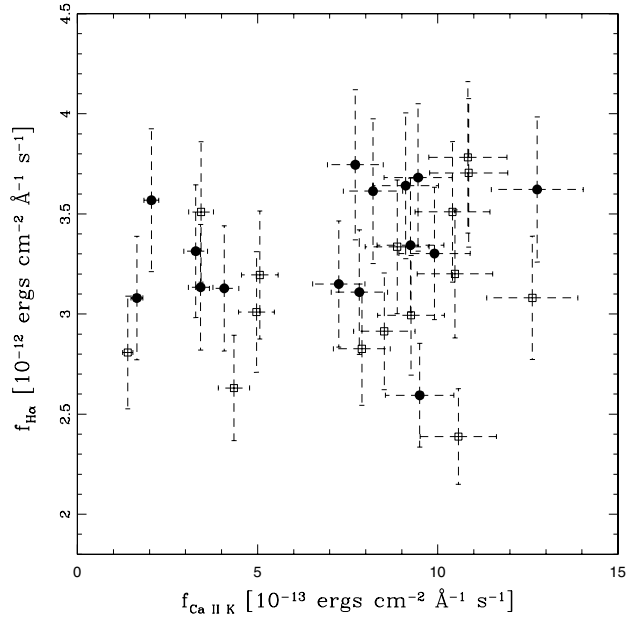


Fig. 9. Line fluxes in H α and in the Ca II K line for the primary (empty squares) and the secondary (filled circles) components of the system. It can be seen that the line fluxes are uncorrelated for both stars. The error bars correspond to a 10% error in the line fluxes.

as activity proxies, such as the Ca II K line. Note that the line fluxes of the primary component are systematically larger than those of the secondary. The mean flux of the primary is around 13% larger than on the secondary, and the difference appears to be greater for larger fluxes.

In Fig. 10 we plot the flux in the K line as a function of time. Distinct maxima are present for both components around the years 2002 and 2004. There are also significant minima at 2001.5 and 2003.5, and a less clear one at around 2006. Apparently, the periods with little activity (minima) are much shorter than those

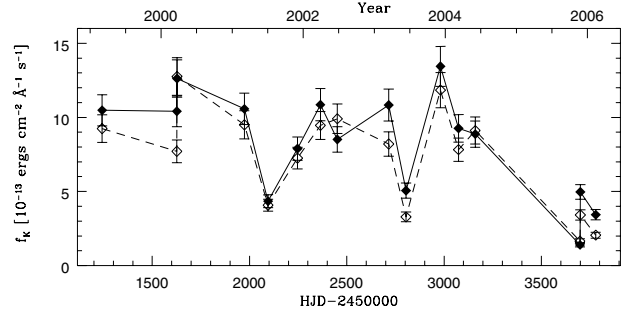


Fig. 10. Flux in the Ca II K line as a function of time for the primary (solid line) and secondary (dashed line) components of the system. The error bars correspond to an 10% error in the line fluxes.

with higher level of chromospheric emission and are separated by about 2 years.

Another activity indicator usually employed in the study of M stars is the flux in H α , which is generally considered to correlate well with the flux in the Ca II H and K lines. It also has the advantage of being located in a redder wavelength range than the Ca II lines, where M dwarfs are brighter. However, it has been recently reported by Cincunegui et al. (2007b) that the correlation between Ca II and H α is not always valid. In that paper, we found that, while some stars exhibit correlations between H α and the Ca II lines, the slopes change from star to star. Furthermore, other stars exhibit anticorrelations and there are also cases where no correlation is present. Therefore, we checked whether a correlation existed for the components of Gl 375. In Fig. 9 we plot the lines fluxes in H α vs. those in the Ca II K line for both components of Gl 375. It can be seen that within the errors, none of the components exhibit any sign of correlation between the lines fluxes, meaning this line cannot be used as an activity indicator for these stars.

In the next section we study in detail whether the system presents a definite activity cycle, like the one present in the Sun. To do this, we compare the three observed magnitudes.

4.4. Periodicity

In Fig. 11 we plot together the three measured quantities: mean magnitude, amplitude of the rotational modulation, and the K line flux. Since the fluxes in the K lines of both components are in phase, we plot the total flux of the system for clarity in the graph. Also to avoid crowding the graph, we have not included the error bars. The K line flux curve has been shifted by 140 days to coincide with the other curves.

This timelag between photometric and magnetic variations has already been observed for stars of different spectral types, from β Com (GOV) to ϵ Eri (K2V), including binary systems like ξ Boo (see, for example, Gray & Baliunas 1995; Gray et al. 1996b,a). In particular, Gray et al. (1996a) show that the time lag between magnetic variations and variations observed in photometry and temperature are anticorrelated with effective temperature (see their Fig. 8). For the coolest star in their sample (ϵ Eri), the time lag of temperature variations is about 0.3 years. The timelag present in the Gl 375 system is comparable to this value.

As mentioned before, the position of the maxima and minima of the mean magnitude and those observed in the amplitude of the rotational modulation coincide very well. It can also be seen that, once displaced, the behaviour of the K line flux also agrees very well with the other two observables. The maximum around the year 2002.5 is present for all curves, along with the minima

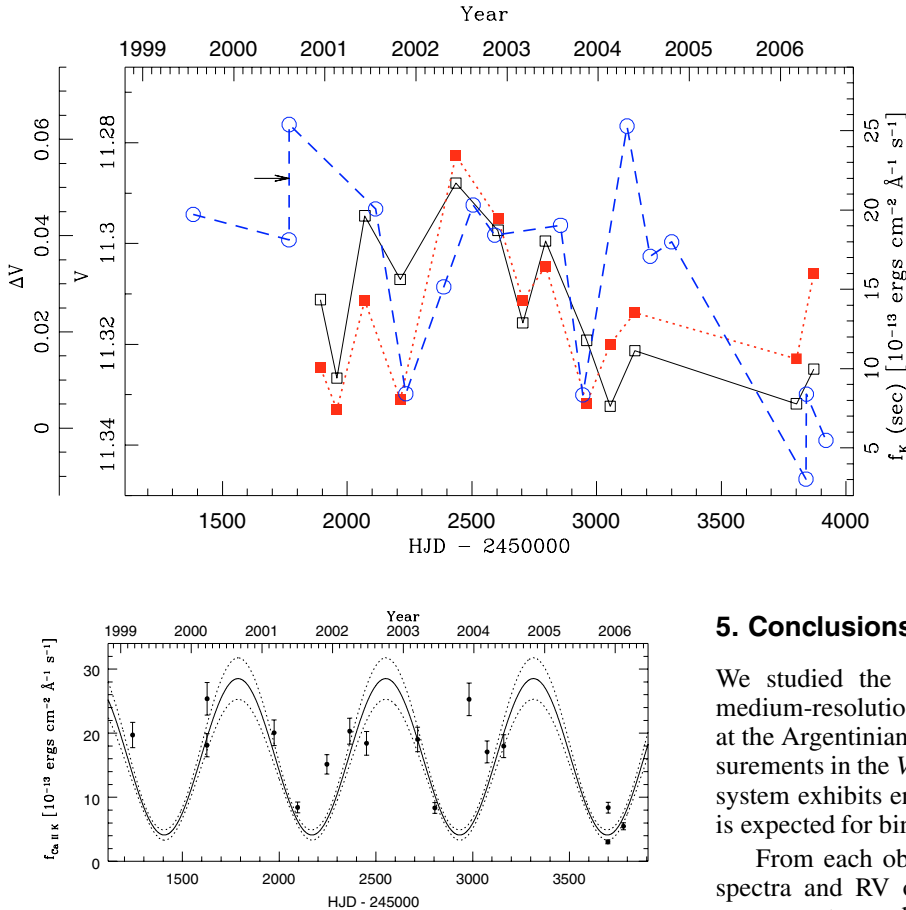


Fig. 12. Total flux of the system in the CaII K line as a function of time. The error bars correspond to a 10% error in the line fluxes, and the solid and dashed lines are the best sinusoidal fit and the $\pm 3\sigma$ deviations, respectively. The period obtained from the fit is 763 days.

near 2001.8 and 2004. Note also (i) that the distinct minimum in the line flux present around the year 2006.2 is also present in the curves of the other two observables, although the minima are much less significant, and (ii) that the slight decrease in magnitude and amplitude around 2003.2 coincides with a decrease in the line flux around 2002.8. Unfortunately, no spectrum was obtained between the one at 2002.8 and the one at 2003.5.

The agreement between the behaviour of the three observables is remarkable, because of both the different nature of the observations and the different instruments and sites in which they were obtained. Although no clear periodicity can be concluded from the present data set, the main minima present in all three curves appear to occur periodically every 2.2 years. This hints at a periodic activity cycle in this system, although more observations are necessary.

To study this point further, we fit the period, amplitude and phase of a sinusoidal function to the total flux using a modification of the Levenberg-Marquardt algorithm available in the SciPy library for Python. The fit is shown in Fig. 12, together with the $\pm 3\sigma$ deviations, for the conservative estimate of 10% in the line fluxes. The obtained period is $P = 763$ days, with a formal error of less than 5 days. However, the fit is extremely sensitive to some of the points. For example, if the lowest point located near $\text{HJD} - 2\,450\,000 = 3700$ is not considered in the fit, the obtained period changes to 786 days. Therefore, we consider that a more realistic error for the period would be about 5%, i.e. about 40 days.

Fig. 11. Mean magnitude (black solid line and empty squares), amplitude of the rotational modulation (red dotted line and filled squares), and flux in the CaII K line (blue dashed line and empty circles) as a function of time. The arrow indicates the temporal displacement of 140 days that has been applied to the line flux (see text).

5. Conclusions

We studied the spectroscopic binary system Gl 375 using medium-resolution *echelle* spectra, obtained since the year 1999 at the Argentinian observatory CASLEO, and photometric measurements in the V band from the ASAS database. We found the system exhibits enhanced levels of chromospheric emission, as is expected for binary systems.

From each observed spectrum, we obtained the individual spectra and RV of each component. We found that the two components are dM3.5 stars and that they orbit each other every ~ 1.88 days in a circular orbit with a minimum radius of $a \sin i \sim 5.7 R_{\odot}$. The minimum masses obtained (see Table 2) are similar to the expected values for this type of star and, therefore, the orbital inclination angle is expected to be $\sim 90^{\circ}$. However, the system does not exhibit eclipses, so we are able to set an upper limit to the inclination angle ($i < 82^{\circ}$), which in turn implies a lower limit for the masses of the components ($M_1 > 0.3646 M_{\odot}$ and $M_2 > 0.3482 M_{\odot}$).

As expected for stars in such a close orbit, their rotational periods are synchronised to the orbital period. This is observed as a modulation in the V-band light curve with the same period as the orbit. Likewise, the amplitude of this modulation is clearly seen to change with time on longer timescales, which we believe is due to differences in the area of the stars covered by the active regions.

Therefore, by studying the evolution of the amplitude of the rotational modulation, we found that the system exhibits a roughly periodic behaviour of 2.2 years (or ~ 800 days). The same period was found in the mean magnitude of the system and in the flux of the Ca II K line, although the Ca flux variations occur 140 days ahead of the photometric ones. This behaviour has been observed previously in other single stars and binary systems, for which the lag between temperature variations and line fluxes was reported to anticorrelate with effective temperature (Gray et al. 1996a). The measured lag for this system fits roughly into that trend, indicating that the same process may be responsible for the phase shift between observables.

The agreement between the behaviour of the three observables is remarkable because of the different nature of the observations and the different instruments and sites where they were obtained. We also performed a non linear fit to the total Ca II K flux using a sinusoidal function and found the

least-square estimation for the period is $P = 763$ days. If confirmed, this would be the second detection of an activity cycle in an M star, the first being a recently reported cycle of around 450 days in Proxima Centauri (Cincunegui et al. 2007a). It is interesting to compare both cases briefly in relation to the 2.5-year lower limit for the period of activity cycles in solar stars given by Baliunas et al. (1995). Although slightly shorter, the period of the Gl 375 system is consistent with this limit, which is reasonable, since Gl 375 A and Gl 375 B are dM3.5 stars that should have a radiative core surrounded by a convective outer envelope. Therefore, in the Gl 375 system the standard dynamo could in principle explain the cyclic behaviour observed, as in the earlier stars included in the study by Baliunas et al. (1995). On the other hand, the period of Proxima Centauri is well below the 2.5-year lower limit. This might be due to the fact that Proxima Centauri is a dM5.5 star and should, therefore, be completely convective. Hence, a different mechanism must be responsible for the production of the activity cycle in Proxima Centauri than in Gl 375 and earlier stars. Further observations of these systems, along with the discovery of activity cycles in other M stars, should provide a solid observational basis for developing a model capable of explaining the observations.

Another interesting result of this work is that the activity of Gl 375 A and Gl 375 B, as measured in the flux of the Ca II K lines, are in phase. The levels of chromospheric emission of both components exhibit an excellent correlation, which implies that a magnetic connection exists between both components, as is shown in numerical simulations by other authors. Due to its vicinity and relative brightness, this system presents an interesting opportunity for further study of this type of interaction.

Finally, since the chromospheric emission is stronger when the system is brighter, which coincides with period of maximum amplitude of the modulation, we conclude that the photometry of these stars is dominated by bright active regions rather than dark spots and that the filling factor is below 50%, very much like in the Sun.

Note added in proof. We have recently become aware of the work by Montes et al. (2006), who derive orbital parameters for this system in good agreement with the ones presented in this work.

Acknowledgements. The CCD and data acquisition system at CASLEO has been partly financed by R. M. Rich through US NSF grant AST-90-15827. This research has made use of the SIMBAD database, operated at the CDS, Strasbourg, France. We would like to thank the CASLEO staff and thankfully acknowledge

the comments and suggestions of the referee that helped us to improve our original manuscript.

References

- Baliunas, S. L., Donahue, R. A., Soon, W. H., et al. 1995, *ApJ*, 438, 269
 Bessel, M. S. 1990, *A&AS*, 83, 357
 Bidelman, W. P. 1985, *ApJS*, 59, 197
 Buccino, A., & Mauas, P. J. D. 2007, in preparation
 Buccino, A. P., Lemarchand, G. A., & Mauas, P. J. D. 2006, *Icarus*, 183, 491
 Buccino, A. P., Lemarchand, G. A., & Mauas, P. J. D. 2007, *Icarus*, accepted [arXiv:astro-ph/0701330]
 Christian, D. J., & Mathioudakis, M. 2002, *AJ*, 123, 2796
 Cincunegui, C., & Mauas, P. J. D. 2004, *A&A*, 414, 699
 Cincunegui, C., Díaz, R. F., & Mauas, P. J. D. 2007a, *A&A*, 461, 1107
 Cincunegui, C., Díaz, R. F., & Mauas, P. J. D. 2007b, *A&A*, 469, 309
 Corben, P. M., Carter, B. S., Banfield, R. M., & Harvey, G. M. 1972, *Monthly Notes of the Astronomical Society of South Africa*, 31, 7
 Cox, A. N. 2000, *Allen's astrophysical quantities*, 4th edn. (New York: AIP Press; Springer), ed. A. N. Cox
 Díaz, R. F., Cincunegui, C., & Mauas, P. J. D. 2007, *MNRAS*, 378, 1007
 Doyle, J. G., & Butler, C. J. 1990, *A&A*, 235, 335
 Doyle, J. G., Mathioudakis, M., Panagi, P. M., & Butler, C. J. 1990, *A&AS*, 86, 403
 Frodesen, A. G., Skjeggstad, O., & Tøfte, H. 1979, *Probability and statistics in Particle Physics* (Universitetsforlaget)
 González, J. F., & Levato, H. 2006, *A&A*, 448, 283
 Gray, D. F., & Baliunas, S. L. 1995, *ApJ*, 441, 436
 Gray, D. F., Baliunas, S. L., Lockwood, G. W., & Skiff, B. A. 1996a, *ApJ*, 465, 945
 Gray, D. F., Baliunas, S. L., Lockwood, G. W., & Skiff, B. A. 1996b, *ApJ*, 456, 365
 Horne, J. H., & Baliunas, S. L. 1986, *ApJ*, 302, 757
 Johnson, H. L. 1965, *ApJ*, 141, 170
 Kirkpatrick, J. D., Henry, T. J., & McCarthy, Jr., D. W. 1991, *ApJS*, 77, 417
 Kron, G. E., Gascoigne, S. C. B., & White, H. S. 1957, *AJ*, 62, 205
 Montes, D., Gálvez, M. C., Fernández-Figueroa, M. J., & Crespo-Chacón, I. 2006, *Ap&SS*, 304, 367
 Perryman, M. A. C., Lindgren, L., Kovalevsky, J., et al. 1997, *A&A*, 323, L49
 Pettersen, B. R., & Hawley, S. L. 1989, *A&A*, 217, 187
 Pojmanski, G. 2002, *Acta Astron.*, 52, 397
 Press, W. H., Teukolsky, S. A., Vetterling, W. T., & Flannery, B. P. 1992, *Numerical recipes in C. The art of scientific computing* (Cambridge: University Press), 2nd edn.
 Reid, I. N., Hawley, S. L., & Gizis, J. E. 1995, *AJ*, 110, 1838
 Scargle, J. D. 1982, *ApJ*, 263, 835
 Schrijver, C. J., & Zwaan, C. 1991, *A&A*, 251, 183
 Udry, S., Bonfils, X., Delfosse, X., et al. 2007, *A&A*, 469, L43
 Vahia, M. N. 1995, *A&A*, 300, 158
 van Altena, W. F., Lee, J. T., & Hoffleit, E. D. 1995, *The general catalogue of trigonometric [stellar] parallaxes* (New Haven, CT: Yale University Observatory), 4th edn., completely revised and enlarged
 von Bloh, W., Bounama, C., Cuntz, M., & Franck, S. 2007, submitted [arXiv:astro-ph/0705.3758]
 Zahn, J.-P. 1977, *A&A*, 57, 383
 Zaqarashvili, T., Javakhishvili, G., & Belvedere, G. 2002, *ApJ*, 579, 810